

# Ion beam synthesis of SiC thin films

Shunichi Hishita

Received: 30 November 2007 / Accepted: 24 July 2008 / Published online: 29 August 2008  
© Springer Science + Business Media, LLC 2008

**Abstract** This report reviews irradiation effects of 2 MeV He<sup>+</sup>, Ne<sup>+</sup>, and Ar<sup>+</sup> ions on the film structure of the carbon-film/Si-substrate system. Using ion irradiation, an epitaxial silicon carbide (SiC) film is grown at atmospheric temperature on a Si substrate. The SiC formation is achieved with appropriate thickness of the initial carbon film. Kinetic analyses of the ion dose dependence of the SiC formation reveal that the SiC film thickness evolution process includes three stages. The first is a steep increase of the SiC, which is governed by inelastic collision. The second is a gentle increase of the SiC, which is governed by diffusion. The last is a decrease of the SiC, which is caused by sputtering. The SiC formation mechanism is also discussed.

**Keywords** Ion beam synthesis · Epitaxial growth · Epitaxial SiC film · Silicon carbide thin film · Electronic stopping power · Nuclear stopping power

## 1 Introduction

Silicon carbide (SiC) is an attractive material for next-generation semiconductors and for high-temperature electronic devices. It has a wide band-gap (2.2 eV), high electron mobility (1000 cm<sup>2</sup>/Vs [1]), high saturated electron drift velocity (calculated as  $2.7 \times 10^7$  cm/s at  $2 \times 10^5$  V/cm)[2], and thermal stability (stable at temperatures greater than 2000 K). To realize SiC devices which have these interesting properties, high-quality SiC thin films must be produced, especially epitaxially grown films on Si substrates. The

growth of epitaxial SiC films on silicon substrates has been reported with high substrate temperatures greater than 1000 K [3–14]. The epitaxial SiC films on silicon substrates have been grown using chemical vapor deposition at 1023–1623 K [3–9]. Wahab et al. reported epitaxial growth of SiC films by reactive magnetron sputtering at 1123 K [10]. The carbonization of silicon by C<sub>60</sub> at 1073–1273 K [11–14] has been examined to grow epitaxial SiC films. Regarding hetero-epitaxial growth of SiC on Si substrates, a key issue related to quality is the process temperature because of the large lattice mismatch (20%) and the difference in the thermal expansion coefficients (8%) between SiC and Si. For that reason, many efforts have been undertaken to reduce the process temperature. An effective process temperature reduction method is to use the ion beam technique. Goto et al. reported the epitaxial growth of SiC films on Si substrates at 900–1300 K using organosilicon ions [15, 16]. Tsubouchi et al. grew epitaxial SiC films using direct irradiation of Si and C ions to Si substrates at 943 K [17]. In those studies, the kinetic energies of Si and C ions were used to reduce the process temperature.

From the viewpoint of energy transfer, the energetic ions and target atoms share two interactions [18]: elastic and inelastic collisions. In an elastic collision, the energetic ion loses its energy by transferring its kinetic energy to the target atom nucleus (nuclear stopping). An inelastic collision transfers the energy to the target atom's electrons (electronic stopping). The author's group has reported the room temperature growth of epitaxial SiC thin films on Si substrates by ion irradiation [19–22]. The key issue of this epitaxial growth of SiC films should be the energy transfer by electronic stopping of high-energy (approximately 2 MeV) ions. Herein, the reported results are summarized and the growth kinetics and mechanisms are discussed along with additional data.

---

S. Hishita (✉)  
Sensor Materials Center, National Institute for Materials Science,  
1-1, Nakimi, Tsukuba, Ibaraki 305-0044, Japan  
e-mail: HISHITA.Shunichi@nims.go.jp

## 2 Epitaxial growth of SiC films by Ar<sup>+</sup> irradiation [19, 20]

The detailed experimental setup is described elsewhere [21]. Non-doped Si single crystals of (100) orientation were used as substrates. To develop cleaned surfaces, all crystals were heated at 1473 K under a vacuum ( $<5 \times 10^{-7}$  Pa) for 1 min after ordinary chemical treatment. The cleaned surface of Si (100) was confirmed as a  $2 \times 1$  reconstruction using RHEED and LEED; no trace contamination was observed using X-ray photoelectron spectroscopy (XPS). Carbon films with thickness of 0.05–50 nm were evaporated onto the Si substrates at 300 K. The thickness of the initial carbon films was determined from the XPS intensity ratio of C 1s and Si 2p peaks; it was calibrated using the RUMP simulation [23] of UHV-Rutherford backscattered (RBS) spectra and with absolute C 1s XPS intensity from the graphite monolayer on Ni (111) [24]. The film thickness determined by RBS and RUMP simulation is given by atoms per square meter unit. So, the carbon film thickness in nm unit was calculated by assuming that the atomic density was equal to that of graphite (1 nm-thick carbon =  $14 \times 10^{19}$  atoms/m<sup>2</sup>). For indicating the atomic population at the interface of the substrate and film, the monolayer (ML) unit is also used to present the film thickness, that is, one ML on the Si(100) is  $0.7 \times 10^{19}$  atoms/m<sup>2</sup>. The thickness values presented in this paper include about 10% error. Irradiation of the samples with 2 MeV Ar<sup>+</sup> was performed with ion current densities of 10 mA/m<sup>2</sup>. The sample temperature was monitored using a thermocouple attached to the side of the sample. The detected temperature increase of during ion irradiation was less than 50 K. The real temperature of the sample under the ion irradiation was estimated not to exceed 400 K, considering the temperature gradient between the sample and the thermocouple. In addition, XPS measurements for SiC growth detection were conducted with Mg K $\alpha$  excitation (Escalab 200-X with an

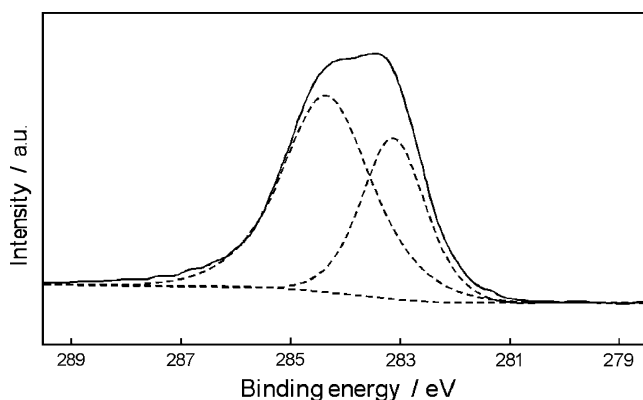


**Fig. 1** C 1s XPS spectrum of the Ar<sup>+</sup> irradiated sample. The thickness of the initial carbon film is about 0.9 nm. The ion dose is  $5.6 \times 10^{19}$  ions/m<sup>2</sup>. The *solid line* is the measured spectrum; the *broken one* is the resolved spectrum

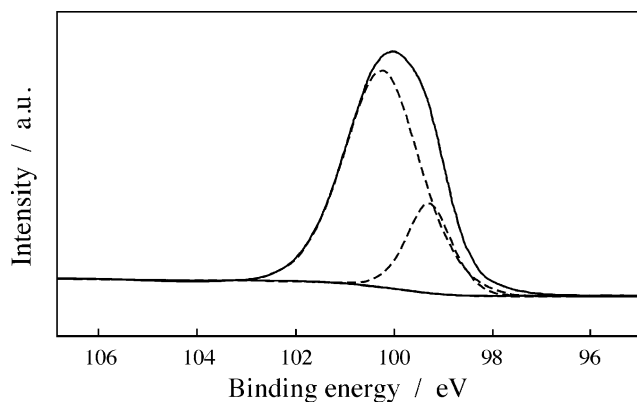


**Fig. 2** Si 2p XPS spectrum of the Ar<sup>+</sup> irradiated sample. The thickness of the initial carbon film is about 1.0 nm. The ion dose is  $1.9 \times 10^{20}$  ions/m<sup>2</sup>. The *solid line* is the measured spectrum; the *broken one* is the resolved spectrum

Eclipse data system; Thermo VG Scientific). The binding energy of XPS spectra was calibrated using the Si 2p peak (99.3 eV [25]) from the "bulk" Si (100) sample. A single crystal SiC (6H; Nippon Steel Corp.) was also used as a reference material.

The RHEED patterns from the as-deposited carbon films over 0.2 nm (4 ML) in thickness showed no visible intensity distribution, indicating that the films were amorphous. The subsequent heating of the amorphous carbon films up to 823 K produced no visible changes in the RHEED pattern. With heating to temperatures greater than 1000 K, the carbon films reacted with the silicon substrate and the cubic (3C) SiC films were grown as reported [26].

During ion irradiation, the RHEED patterns and the XPS spectra of the samples changed drastically. Figure 1 portrays the C 1s XPS spectrum of the sample irradiated with the dose of  $5.6 \times 10^{19}$  ions/m<sup>2</sup>. The initial carbon thickness of the sample shown in Fig. 1 is about 0.9 nm (18 ML). The C 1s peak can be resolved into two components: one peak is centered at 284.4 eV; the other is at 283.1 eV. The former can be assigned to amorphous carbon. The latter is identical to that of the single crystal SiC ( $283.2 \pm 0.2$  eV). The former peak's intensity decreased with increased ion dose. The Si 2p XPS spectra of the samples usually showed interference by the intense peak of the bulk Si (the substrate). A chemical shift of the Si 2p XPS peak was found in the spectrum, as shown in Fig. 2, when the carbon thickness was 1.0 nm (20 ML) and the irradiation dose was  $1.9 \times 10^{20}$  ions/m<sup>2</sup>. The peak centered at 99.3 eV is that of the bulk Si (the substrate); the peak at 100.2 eV should be identical to that of the single crystal SiC ( $100.6 \pm 0.3$  eV). These XPS results indicate that the chemical reaction between C and Si can be excited and that Ar<sup>+</sup> irradiation formed a chemical bond for SiC.

The RHEED patterns from the irradiated samples below  $1.0 \times 10^{20}$  ions/m<sup>2</sup> showed no visible changes. Diffuse spots appeared when the ion dose exceeded the threshold, which

was dependent on the initial carbon thickness; the spots were sharpened, as shown in Fig. 3 with the increasing ion dose amount. The spot patterns depicted in Fig. 3 indicate that the fcc crystallite grows epitaxially. The lattice constant calculated from the spacing of the spots using the Si (100) spacing as a reference was about 0.43 nm, which was identical to that of cubic (3C) SiC ( $a=0.43589$  nm).

The C 1s XPS peak position and the crystallization of the film on the Si substrate are presented schematically in Fig. 4 for the 0.1-nm-thick (2 ML) carbon films. The ion irradiation excites the reaction between carbon and silicon, and the Si-C bond is formed, i.e., the formation of amorphous SiC. The amorphous SiC is grown epitaxially using further irradiation at ambient temperature. The epitaxial relationship between the SiC film and the substrate was  $(100)_{\text{SiC}} // (100)_{\text{Si}}$  and  $[001]_{\text{SiC}} // [001]_{\text{Si}}$ .

The surface structure of the irradiated sample is dependent on the initial thickness of the carbon film. For 1.5-nm-thick (30 ML) carbon films, the dose of  $7.5 \times 10^{20}$  ions/m<sup>2</sup> is necessary for the SiC films' epitaxial growth. The turbostratic structure is grown at the film surface, as shown in Fig. 5 with the dose greater than  $5 \times 10^{19}$  ions/m<sup>2</sup> when the thickness is greater than 2.5 nm (50 ML). The C 1s peak position (284.3 eV) in XPS spectra and the calculated lattice constants

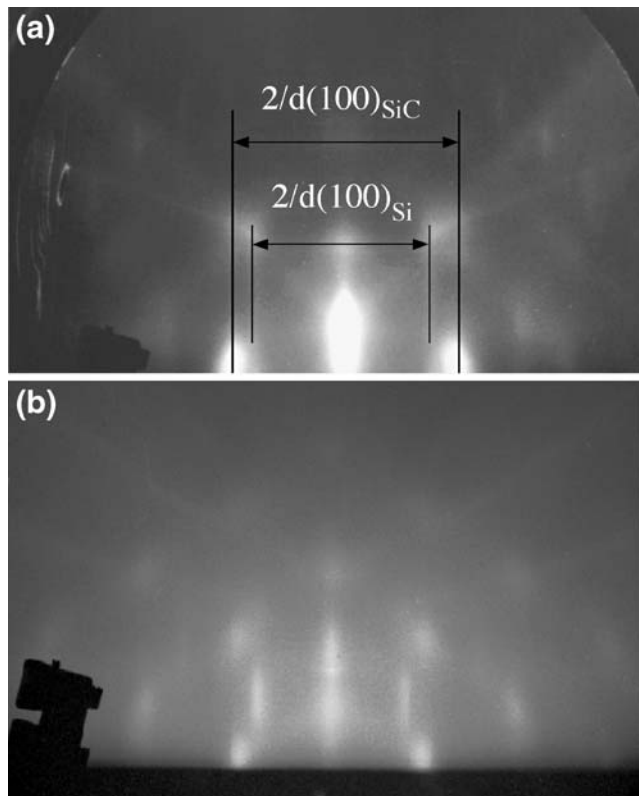


**Fig. 3** RHEED pattern of the Ar<sup>+</sup> irradiated sample. The azimuth of the incident electron beam respectively shows (a) [110] and (b) [110] directions of the Si substrate. The initial carbon thickness is about 0.1 nm; the ion dose is  $2.8 \times 10^{20}$  ions/m<sup>2</sup>

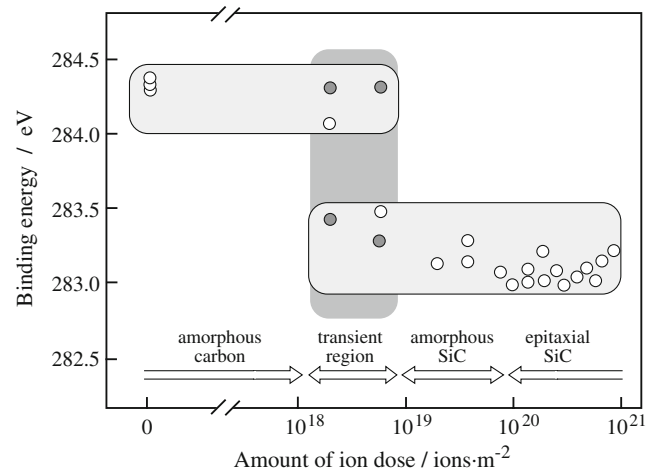


**Fig. 4** Effect of the amount of Ar<sup>+</sup> ion dose on the C 1s XPS peak position. The initial carbon thickness is about 0.1 nm; solid circles are obtained by peak resolution

( $a=0.23$ ,  $c=0.67$  nm) from Fig. 5 indicate that the turbostratic graphite ( $a=0.2456$ ,  $c=0.6696$  nm) is formed at the carbon film surface at ambient temperature by 2 MeV Ar<sup>+</sup> ion irradiation. The formation of SiC was also detected from the Si 2p peak position in the XPS spectrum of the sample which initial carbon thickness was 2.5 nm (50 ML) and was irradiated at  $5 \times 10^{19}$  ions/m<sup>2</sup>. So, the SiC film is considered to be formed at the interface of the carbon film and the substrate when the turbostratic graphite is grown. The thickness-dose-dependence of the film surface structure during 2 MeV Ar<sup>+</sup> ion irradiation is summarized schematically in Fig. 6.

### 3 Epitaxial growth of SiC films by He<sup>+</sup> and Ne<sup>+</sup> irradiation [21, 22]

Irradiation of the samples with 2 MeV He<sup>+</sup> and Ne<sup>+</sup> was performed respectively with ion current densities of 20 and

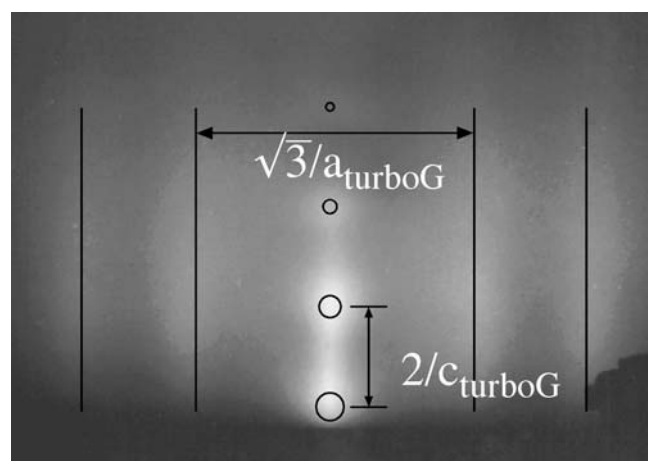


**Fig. 5** RHEED pattern of the turbostratic graphite. The initial carbon thickness is about 3.5 nm; the ion dose is  $9 \times 10^{19}$  ions/m<sup>2</sup>

10 mA/m<sup>2</sup>. Some samples were irradiated at 623 K to verify the heating effect because of the difference in the ion-current density. However, no detectable effect of heating was found among the samples under the ion-current density examined.

The RHEED patterns and the XPS spectra indicated the formation of epitaxial SiC thin films by irradiation of 2 MeV He<sup>+</sup> and Ne<sup>+</sup> ions, as well as the case of Ar<sup>+</sup> ion irradiation, when the thickness of the initial carbon films was appropriate. The epitaxial growth of SiC by He<sup>+</sup> irradiation was observed in samples with initial carbon film thickness of less than 0.07 nm (1.4 ML). When the thickness was greater than 0.08 nm (1.6 ML), the RHEED pattern of the samples showed no visible change by He<sup>+</sup> irradiation, indicating amorphous SiC. The critical thickness of the initial carbon film for growing the epitaxial SiC thin film was increased in the order of He<sup>+</sup> (0.07 nm=1.4 ML), Ne<sup>+</sup> (0.3 nm=6 ML), and Ar<sup>+</sup> (2 nm=40 ML).

#### 4 SiC film growth kinetics and formation mechanisms

The amount of formed SiC was used to analyze the growth kinetics and formation mechanism of SiC films by ion irradiation from the viewpoint of atomic reaction that included the formation of SiC islands. The amount of SiC was calculated from the C 1s XPS spectrum. The energy positions of the resolved C 1s peaks were independent of the ion dose and the initial carbon thickness, as shown in Fig. 4, indicating the presence of two chemical states of the carbon: amorphous carbon; and that reacted with Si, so-called SiC carbon. The carbon atoms in irradiated films are in either of

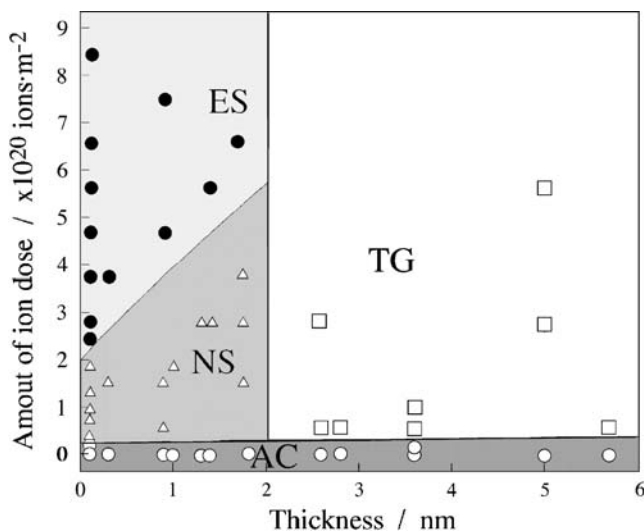


**Fig. 6** Effects of carbon film thickness and the Ar<sup>+</sup> ion dose amount on the film structure. ES (solid circles), epitaxial SiC; AS (triangles), amorphous SiC; TG (squares), turbostratic graphite; AC (open circles), amorphous carbon

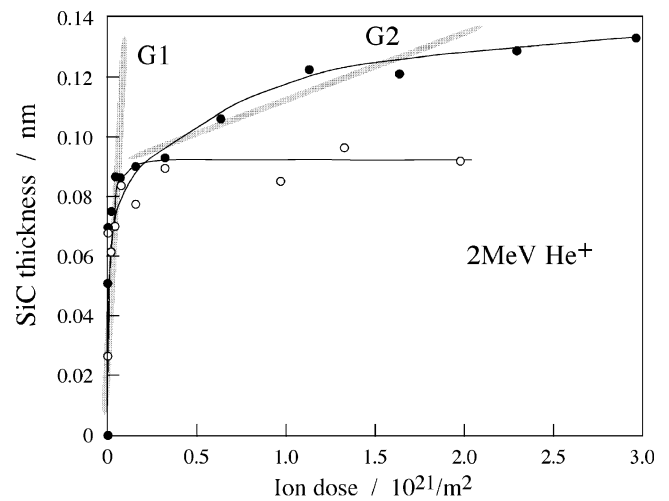


**Fig. 7** He<sup>+</sup> ion dose-dependence of SiC film thickness. Initial carbon thicknesses are 0.17 nm for solid circles and 0.08 nm for open circles

these two states, independent of the amount of ion dose or the initial film thickness. The amount of SiC is calculated from the peak area ratio of SiC carbon to amorphous one in the C 1s XPS spectrum: The total carbon atoms on the substrate can be determined from the intensity ratio of C 1s and Si 2p peaks. The amount of SiC carbon in atoms per square meter unit is calculated from the peak area ratio of SiC carbon and amorphous one by assuming that the XPS intensity factor for carbon in SiC is identical to that for pure carbon. Thus, the calculated value of SiC carbon in atoms/m<sup>2</sup> unit is equal to the amount of SiC “molecule” in molecules per square meter unit, which means, for example, 1 ML SiC carbon is equal to 1 ML SiC “molecule”. For simplifying the

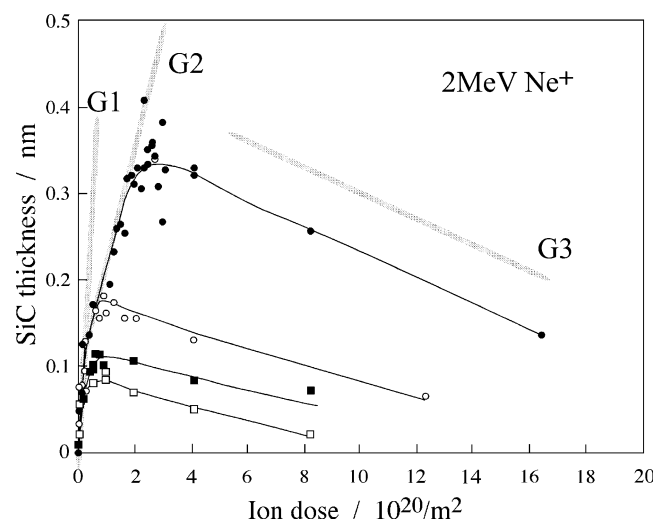


**Fig. 8** Ne<sup>+</sup> ion dose-dependence of SiC film thickness. The initial carbon thicknesses are 0.85 nm for the solid circles, 0.25 nm for open circles, 0.15 nm for solid squares, and 0.1 nm for open squares

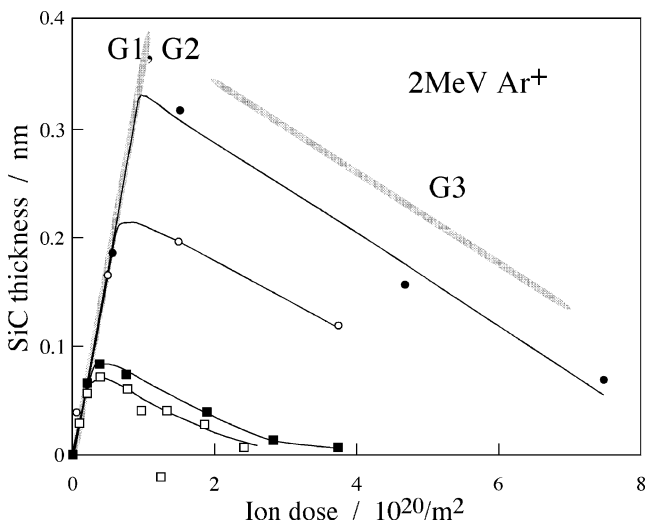


**Fig. 9** Ar<sup>+</sup> ion dose-dependence of SiC film thickness. The initial carbon thicknesses are 0.9 nm for *solid circles*, 0.6 nm for *open circles*, 0.13 nm for *solid squares*, and 0.1 nm for *open squares*

discussion bellows, hereafter the thickness of SiC film is presented as an equivalent value to that of carbon film, that is, 1 nm-thick SiC means the SiC film consisted of  $14 \times 10^{15}$  atoms/cm<sup>2</sup> (1 nm-thick) carbon and Si.

Figures 7, 8 and 9 portray the evolution of the thickness of SiC films with the amount of the ion dose. The thickness of initial carbon films was also varied. For He<sup>+</sup> irradiation (Fig. 7), the evolution process is divisible into two stages. The SiC film thickness increased steeply to about 0.08 nm (1.6 ML), followed by saturation to about 0.13 nm (2.6 ML), even though the initial carbon thickness was greater than 0.13 nm (2.6 ML). This pattern of increase and saturation indicates that the carbon atoms in the layer of about 0.13 nm (2.6 ML) thickness react with Si atoms to form the SiC film by 2 MeV He<sup>+</sup> irradiation. For Ne<sup>+</sup> irradiation (Fig. 8), the evolution process is divisible into three stages. The thickness of SiC films was steeply increased to about 1 nm (20 ML), which subsequently increased slowly, and decreased linearly. For Ar<sup>+</sup> irradiation (Fig. 9), the evolution process is divisible into two stages. The thickness of SiC films was increased first, followed by decreasing. Comparison of the dose amount to that in the

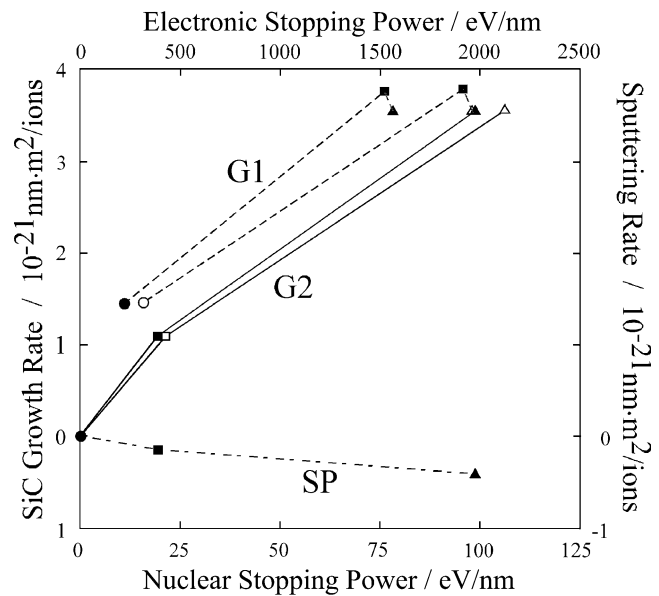


**Fig. 10** Relationship between the SiC growth rate and the transferred energy. The *broken line* (G1) represents the electronic energy transfer. The *solid line* (G2) shows the nuclear energy transfer. The *dashed line* (SP) shows sputtering. The *solid symbols* are for Si, and the *open ones* are for C. The *circles* denote He<sup>+</sup>, the *triangles* denote Ne<sup>+</sup>, and the *squares* denote Ar<sup>+</sup>

case of Ar<sup>+</sup> irradiation suggested that the experimental setup and procedure had less capability for distinguish the two-stage increasing process of SiC thickness, as shown in the He<sup>+</sup> and Ne<sup>+</sup> cases. For that reason, the evolution process of SiC film thickness is thought to comprise three stages: a steep increase (abbreviated as G1), a gentle increase (G2), and a linear decrease (SP). During the decrease, the amount of total carbon was also decreased, which indicates that sputtering causes the decrease process.

The energy for the SiC formation should be supplied by the irradiated ions. The total energy transferred from the irradiated ion is a sum of the nuclear (elastic collision) and electronic (inelastic collision) contributions. The nuclear contribution is related to the displacement of C and Si atoms, i.e. sputtering and/or diffusion; the electronic one is to the excitation of the Si-C bond formation. The energy transferred from the ions to the C-Si system was estimated using the Monte Carlo simulation code TRIM [27] for a

**Table 1** Energy values transferred from one 2 MeV-ion and the sputtering rate.

	Electronic energy (eV/nm) to		Nuclear energy (eV/nm) to		Sputtering rate (N/nm) for	
	C	Si	C	Si	C	SiC
He <sup>+</sup>	318	233	0.262	0.239	0.0008	0.0002
Ne <sup>+</sup>	1916	1522	21.58	19.83	0.1	0.02
Ar <sup>+</sup>	1962	1568	106.5	98.79	0.3	0.08

carbon film of 1 nm (20 ML) in thickness on a Si film of 10  $\mu\text{m}$  and for a “bulk” SiC. The estimated values are listed in Table 1. The sputtering rate was calculated from the vacancy generation process with the assumption that the displacement energies were 28 eV for C and 15 eV for Si, and that the lattice binding energy was 3 eV. The sputtering rates shown in Table 1 are consistent with the results shown in Figs. 7, 8 and 9: the SiC thickness was not decreased for  $\text{He}^+$  irradiation, but it gently decreased for  $\text{Ne}^+$  irradiation and steeply decreased for  $\text{Ar}^+$  irradiation. Figure 10 shows the correlation between the SiC film growth rate and the transferred energy. The growth rate was estimated from the slope of the G1 or G2 regions in Figs. 7, 8 and 9. The slope of G1 for  $\text{Ar}^+$  irradiation was assumed to be identical to that of G2. The  $\text{He}^+$  irradiation can grow the epitaxial SiC when the initial carbon film is sufficiently thin, which suggests that the electronically transferred energy is the dominant one for initiating the reaction between carbon and silicon and growing the epitaxial film. This is consistent with the G1 lines shown in Fig. 10. The G1 and G2 lines are not corrected by the sputtering effect (SP). When the correction values, which are 0.0, 0.14 and  $0.41 \times 10^{-21}$   $\text{nm}^2/\text{ions}$  for  $\text{He}^+$ ,  $\text{Ne}^+$  and  $\text{Ar}^+$  irradiation, respectively, are added, the G1 lines would indicate the better linear relationship between the SiC growth rate and the electronically transferred energy. The electronically transferred energy to C atoms might be more dominant for the G1 process because of the better linearity of its G1 line. For the G2 process, however, the nuclear energy transfer is indicated to have a dominant contribution.

The formation mechanism of the SiC film can be considered as follows: The high energy ions irradiated to the carbon film on Si substrates transfer the energy to the C and Si atoms by the inelastic collision (the electronic stopping). The atoms reach the excitation state. If the excited C atom and Si atom are mutually adjacent, the excitation state is relaxed by making the C-Si bond, i.e. SiC formation. This process is the G1 process. The formation of SiC occurs only at the interface of the carbon film and the Si substrate. The outer C atoms in the carbon film are not adjacent to the Si atoms in the substrate when the carbon thickness is rather large. The C atoms (or the Si atoms) are forced to diffuse to the partner atom. The diffusion energy is supplied by the elastic collision (the nuclear stopping). Consequently, the diffusion process governs the formation of SiC. This is the G2 process. The growth of the turbostratic graphite reported in [19] should be the other way for relaxation. The excited C atoms not reaching the partner Si atom encounter the other C atom on the diffusion path, and make the C-C bond become graphite. The absence of graphite formation in  $\text{He}^+$  irradiation supports the existence of this graphite-formation mechanism.

## 5 Conclusions

The epitaxial SiC film can grow at atmospheric temperature by ion irradiation of a carbon film on the Si substrate. The SiC film formation is dependent on the thickness of the initial carbon film and the irradiation ion dose. Kinetic analyses of the SiC film formation indicate that the evolution process of the SiC film thickness comprises three stages. The first stage is the sharp increase of the SiC. The second is the gentle increase of the SiC. The last is the decrease of the SiC, and is caused by sputtering. The electronically transferred energy is indicated to be the dominant one for SiC formation. The nuclear energy transfer process, however, makes an important contribution to atomic diffusion, which is the dominant process for SiC formation when the carbon thickness is great.

## References

1. W.E. Nelson, F.A. Halden, A. Rosengreen, *J. Appl. Phys.* **37**, 333 (1966). doi:10.1063/1.1707837
2. D.K. Ferry, *Phys. Rev. B* **12**, 2361 (1975). doi:10.1103/PhysRevB.12.2361
3. K. Takahashi, S. Nishino, J. Saraie, *J. Electrochem. Soc.* **139**, 565 (1992). doi:10.1149/1.2069122
4. W. Bahng, H.J. Kim, *Thin Solid Films* **290–291**, 181 (1996). doi:10.1016/S0040-6090(96)09193-6
5. K.-W. Lee, K.-S. Yu, J.-H. Boo, Y. Kim, T. Hatayama, T. Kimoto et al., *J. Electrochem. Soc.* **144**, 1474 (1997). doi:10.1149/1.1837614
6. Y.H. Seo, K.S. Nahm, E.-K. Suh, H.J. Lee, Y.G. Hwang, *J. Vac. Sci. Technol. A* **15**, 2226 (1997). doi:10.1116/1.580538
7. J.-H. Boo, D.-C. Lim, S.-B. Lee, K.-W. Lee, M.M. Sung, Y. Kim et al., *J. Vac. Sci. Technol. B* **21**, 1071 (2003). doi:10.1116/1.1585073
8. D.-C. Lim, H.-G. Jee, J.W. Kim, J.-S. Moon, S.-B. Lee, S.S. Choi et al., *Thin Solid Films* **459**, 7 (2004). doi:10.1016/j.tsf.2003.12.140
9. Y. Abe, J. Komiyama, S. Suzuki, H. Nakanishi, *J. Cryst. Growth* **283**, 41 (2005). doi:10.1016/j.jcrysgro.2005.05.047
10. Q. Wahab, R.C. Glass, I.P. Ivanov, J. Birch, J.-E. Sundgren, M. Willander, *J. Appl. Phys.* **74**, 1663 (1993). doi:10.1063/1.354818
11. A.V. Hamz, M. Balooch, M. Moalem, *Surf. Sci.* **317**, L1129 (1994). doi:10.1016/0039-6028(94)90279-8
12. S. Henke, B. Stritzker, B. Rauschenbach, *J. Appl. Phys.* **78**, 2070 (1995). doi:10.1063/1.360184
13. D. Chen, R. Workman, D. Sarid, *Surf. Sci.* **344**, 23 (1995). doi:10.1016/0039-6028(95)00840-3
14. L. Aversa, R. Verucchi, A. Boschetti, A. Podesta, P. Milani, S. Iannotta, *Mater. Sci. Eng. B* **101**, 169 (2003). doi:10.1016/S0921-5107(02)00703-1
15. T. Matsumoto, M. Kiuchi, S. Sugimoto, S. Goto, *Surf. Sci.* **493**, 426 (2001). doi:10.1016/S0039-6028(01)01249-3
16. M. Kiuchi, T. Matsutani, T. Takeuchi, T. Matsumoto, S. Suhimoto, S. Goto, *Surf. Coat. Tech.* **177–178**, 260 (2004). doi:10.1016/j.surfcoat.2003.09.003
17. N. Tsubouchi, A. Chayahara, Y. Mokuno, A. Kinomura, Y. Horino, *Appl. Surf. Sci.* **212–213**, 920 (2003). doi:10.1016/S0169-4332(03)00091-6

18. J.F. Ziegler, J.P. Biersack, U. Littmark, *The Stopping and Range of Ions in Solids* (Pergamon Press, New York, 1985), p. 5
19. S. Hishita, K. Oyoshi, S. Suehara, T. Aizawa, Nucl. Instrum. Methods Phys. Res. **B148**, 549 (1999)
20. S. Hishita, K. Oyoshi, S. Suehara, T. Aizawa, Key Eng. Mater. **169–170**, 179 (1999)
21. S. Hishita, T. Aizawa, S. Suehara, H. Haneda, Appl. Surf. Sci. **169–170**, 296 (2001). doi:[10.1016/S0169-4332\(00\)00677-2](https://doi.org/10.1016/S0169-4332(00)00677-2)
22. S. Hishita, T. Aizawa, S. Suehara, H. Haneda, JAERI-Conf 2003-001, 223 (2003)
23. L.R. Doolittle, Nucl. Instrum. Methods Phys. Res. B **9**, 344 (1985). doi:[10.1016/0168-583X\(85\)90762-1](https://doi.org/10.1016/0168-583X(85)90762-1)
24. T. Aizawa, R. Souda, Y. Ishizawa, H. Hirano, T. Yamada, C. Oshima, Surf. Sci. **237**, 194 (1990). doi:[10.1016/0039-6028\(90\)90531-C](https://doi.org/10.1016/0039-6028(90)90531-C)
25. J.F. Moulder, W.F. Stickle, P.E. Sobol, K.D. Bomben, *Handbook of X-ray Photoelectron Spectroscopy* (Physical Electronics, Minnesota, 1995), p. 57
26. J.-S. Luo, W.-T. Lin, Appl. Phys. Lett. **69**, 916 (1996). doi:[10.1063/1.116942](https://doi.org/10.1063/1.116942)
27. J.F. Ziegler, J.P. Biersack, SRIM 2006.01 (2006)